

A Molecular Insight Into Complement Evasion by the Staphylococcal Inhibitor SCIN

Daniel Ricklin, Apostolia Tzekou, Brandon L. Garcia, Michal Hammel, William J. McWhorter, Georgia Sfyroera, You-Qiang Wu, V. Michael Holers, Andrew P. Herbert, Paul N. Barlow, Brian V. Geisbrecht, John D. Lambris

Supplementary Figures

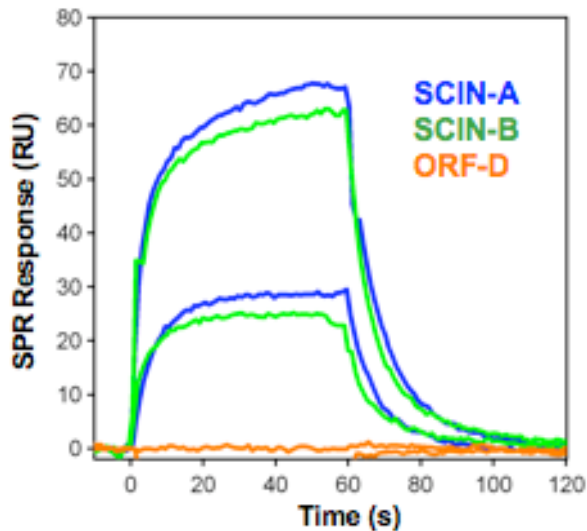


Figure S1. Specificity and activity of individual members of the SCIN family for C3b. While SCIN-A (blue) and SCIN-B (green) bind with similar activity to C3b, no binding could be detected for the reportedly inactive ORF-D (orange). An overlay of two concentrations (125 nM, 500 nM) is shown.

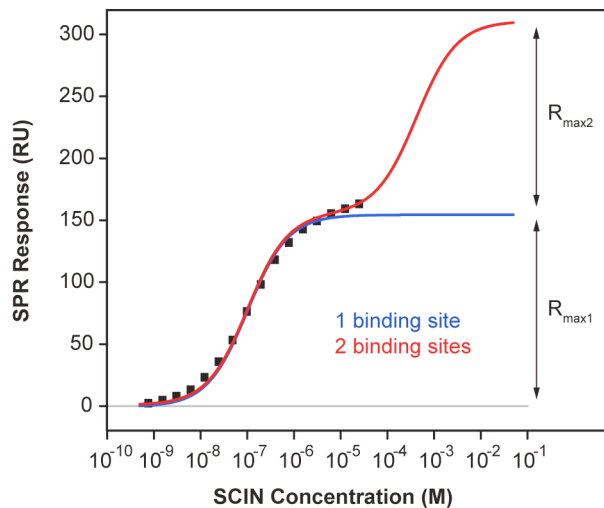


Figure S2. Comparison of different interaction models for SCIN to C3b. Although the steady state data of SCIN (1 nM – 20 μ M) follow a single-binding-site model at lower concentration, the deviation is larger for concentrations above 1 μ M (blue curve). When two distinct binding sites are considered (2:1 model; red curve), the fit does largely improve. Using this extrapolated model, a primary binding site of \sim 100 nM and a secondary site of \sim 200-300 μ M can be extracted. The same maximum binding capacity (R_{max}) was assumed for both binding sites in the 2:1 model.

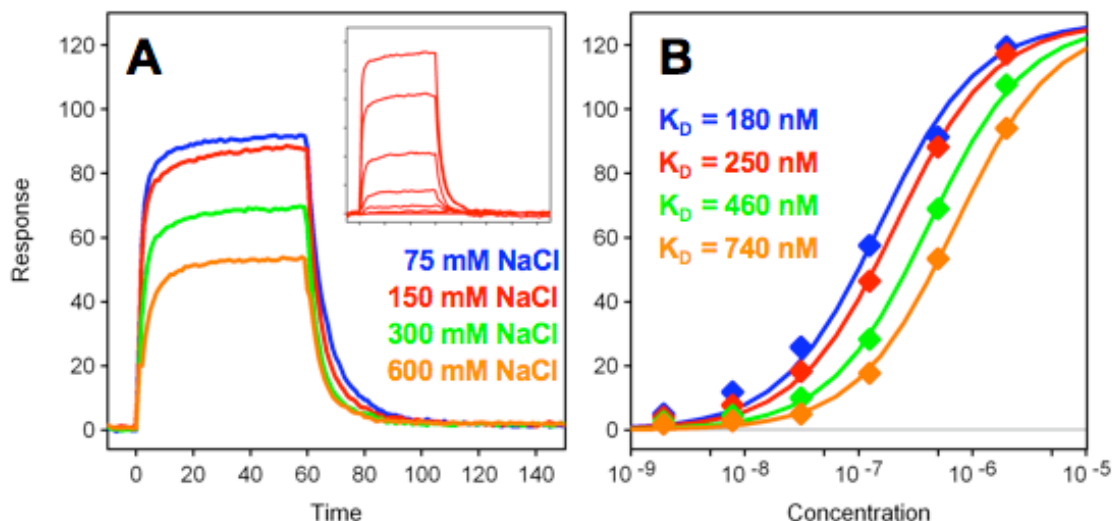


Figure S3. Effects of buffer ionicity on the binding of SCIN to C3b. Increasing amounts of NaCl (75-600 mM) in the PBS buffer decreased the binding affinity of SCIN (2 nM-2 μ M), which indicates a significant contribution of electrostatic effects on the interaction. **A**, Overlay of 500 nM SCIN for all buffer strengths. A full data set for PBS with 150 mM NaCl is shown in the insert. **B**, The steady state responses of all data sets were globally fit to a single-binding-site model and revealed a trend for decreasing affinity with increasing salt concentrations.

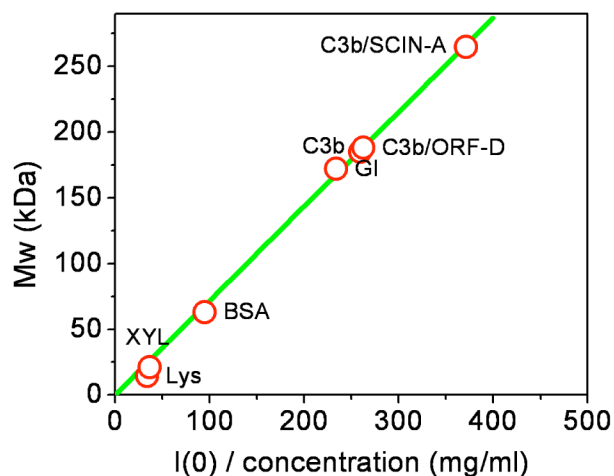


Figure S4. Plot of observed Mw versus concentration-normalized, zero-angle scattering intensity ($I(0)$). The molecular weights of C3b, C3b-ORF-D and C3b-SCIN-A were determined by extrapolating each sample intensity at the zero angle and comparing the value to a standard curve derived from four reference proteins (Lysozyme (LYS), Xylanase (XYL), Bovine serum albumin (BSA), Glucose Isomerase (GI) [39].

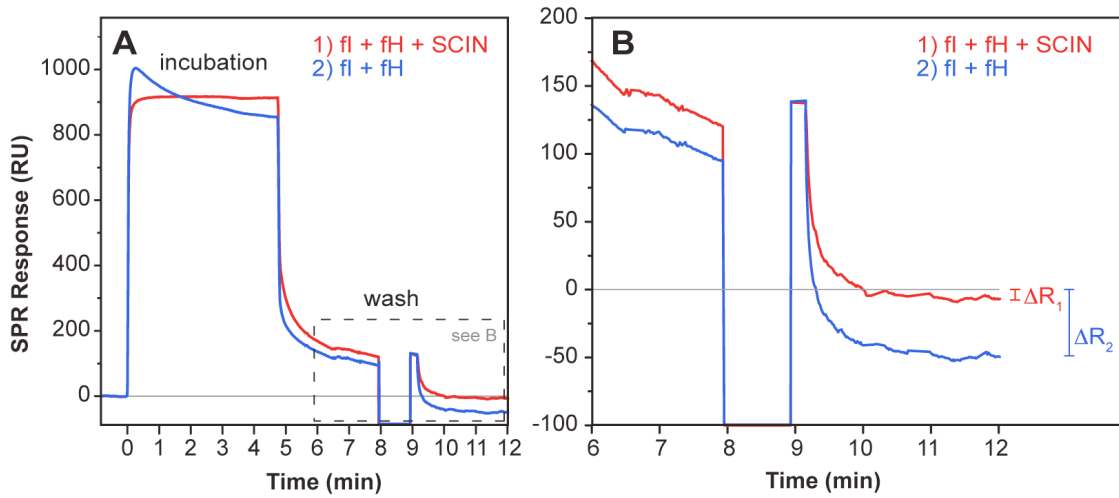


Figure S5. Conversion of C3b to iC3b by fH and fl in presence or absence of SCIN. (A) Thioester-specifically immobilized C3b was first incubated for 5 min with a mixture of fl and fh in the presence of SCIN (red) and the surface was washed with NaCl. In this case, the signal remained stable during incubation and the drop in post-wash baseline was very low. When the same cycle was repeated in absence of SCIN (blue), a significant drift in the incubation signal and a clear drop in baseline can be observed, which indicates cleavage to iC3b. (B) A closer look at the baseline drop after incubation and wash reveals that the first drop (ΔR_1) was ~ 5 RU whereas the second drop was some 40 RU (ΔR_2). When considering the immobilization density of C3b (~ 3000 RU; MW=175 kDa), this difference closely corresponds to the mass loss (2.02 kDa; 35 RU) expected during conversion to iC3b.

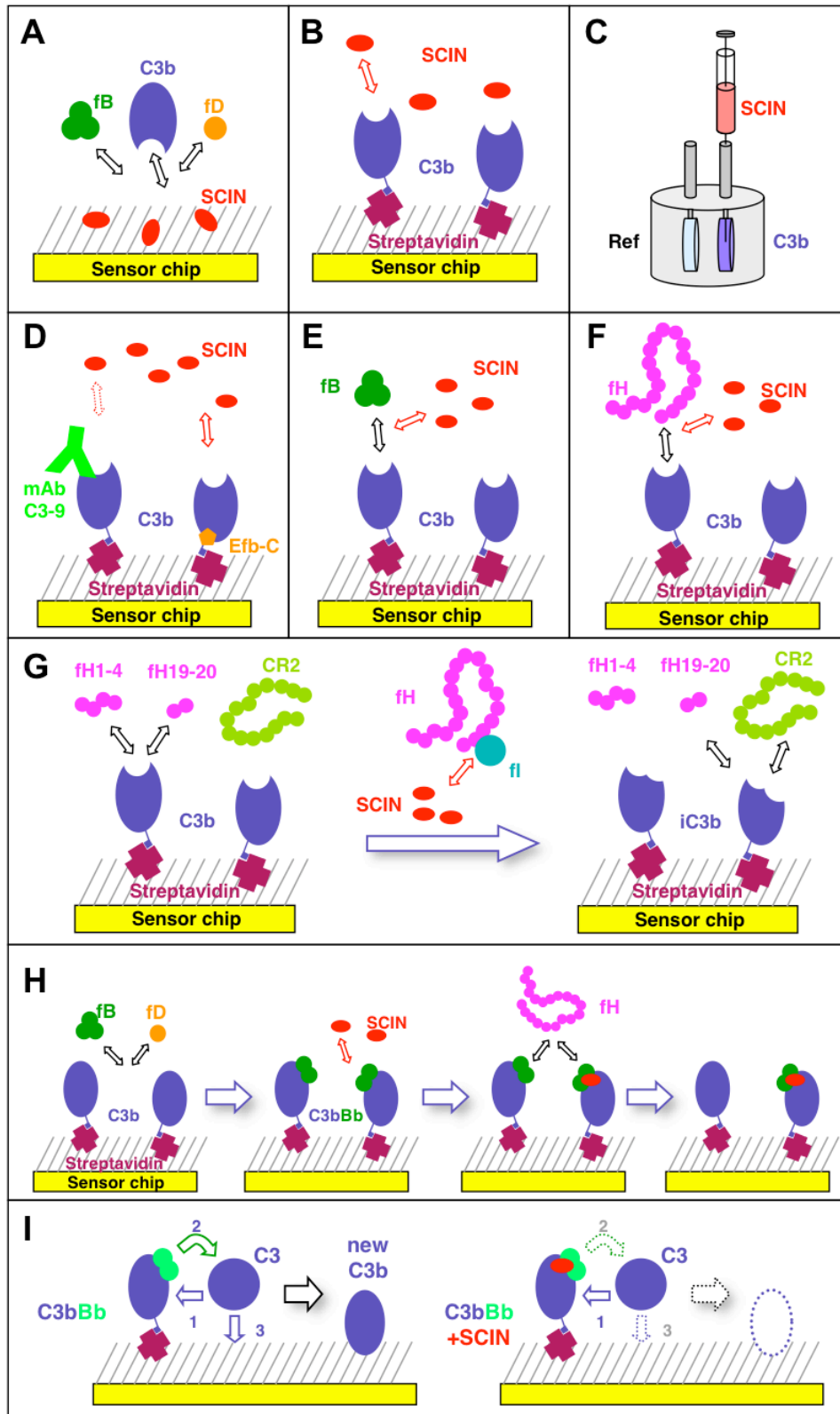


Figure S6: Schematic representations of the direct binding assays using randomly coupled SCIN (A; see Fig. 1A) or site-specifically immobilized C3b (B; see Fig. 1B-D), ITC assay (C; see Fig. 1E+F), mAb blocking assay (D; see Fig. 3A), competition assays for fB (E; see Fig. 4A) and fH (F; see Fig. 4B), surface-based co-factor assay (G; see Fig. 5), on-chip convertase formation/stability assay (H; see Fig. 6), and convertase activity assay (I; see Fig. 7).